Biophysical Journal, Volume *115*

Supplemental Information

Dynamics of Chromatin Fibers: Comparison of Monte Carlo Simulations with Force Spectroscopy

Davood Norouzi and Victor B. Zhurkin

Dynamics of Chromatin Fibers:
Comparison of Monte Carlo Simulations with Force Spectroscopy

Davood Norouzi and Victor B. Zhurkin
Laboratory of Cell Biology, CCR, National Cancer Institute, NIH, Bethesda, MD, USA

Supporting Materials

Energy terms and geometry

Schematic description of the DNA and fiber geometry, Monte Carlo moves, and energy terms are depicted in Figure S1.

(**I**) DNA Elastic energy. The elastic energy of the linker DNA deformation is calculated using the knowledge-based potential functions introduced by Olson et al. [32]. The stiffness constants, f_{ij}, including the cross correlations (such as Twist-Roll) are taken as averages for all 16 dinucleotides. As the rest-state values, $\bar{\theta}_i$, we use the average helical parameters of B-DNA: Twist = 34.5° and Rise = 3.35 Å.

$$E = \tfrac{1}{2} \sum_{i=1}^{6} \sum_{j=1}^{6} f_{ij}(\theta_i - \bar{\theta}_i)(\theta_j - \bar{\theta}_j)$$

(**II**) Electrostatic energy. The electrostatic energy is calculated using the Coulomb potential with 30 Å distance cutoff with charges subject to salt screening. We chose partial charges in such a way that the nucleosome remains 'slightly' negatively charged, which is consistent with electrophoresis experiments [S2]. The centers of charges considered in our calculations are: Cz, Nz in Arginine and Lysine with corresponding partial charge +1; Cd, Cg in Glutamate and Aspartate with partial charge –1, and the Phosphate (P) atoms in nucleosomal DNA with partial charge –0.3. This level of neutralization is predicted in numerical computations [S3]. The long and flexible tails of H3 histones were cut away, but their effect has been taken into account implicitly. According to recent MD simulations [S4] the

positively charged H3 tails are likely to align along the linkers, resulting in a significant neutralization of linker DNA. Linker DNA was modeled with the partial charges –0.25 per nucleotide.

We made a comparison between energy profiles obtained by the truncated Coulomb potential and the Debye-Huckel potential previously [30]. We showed that changing the details of electrostatic potential does not change quantitatively the optimal energy profiles. We chose this interaction because, in compact structures with solvent being pushed out of the crowded regions the electrostatic interactions are stronger locally and decay faster outside a cutoff range.

(**III**) Steric clashes. Steric clashes are modeled by a repulsive van der Waals potential. All the centers of charges considered above are included here, as well as the centers of the DNA base pairs (shown as gray circles in Fig. S1). The van der Waals radii are assumed to be 3.0 Å for the centers of charges and 8.0 Å for the DNA base pair centers. The potential is the repulsive part of the Lennard-Jones potential calculated as:

$$E_{vdW} = 4\varepsilon \times \sum_{i<j} \left(\frac{\sigma_i + \sigma_j}{r_{ij}}\right)^{12}$$

where ε = 2.5 kT, σ_i, σ_j are the van der Waals radii, and r_{ij} is the distance between the corresponding pseudo-atoms.

(**IV**) H4 tail – acidic patch interactions. The attractive interactions between the H4 tail and the acidic patch are modeled phenomenologically [30]. We calculate the distance, "*r*", between the H4 tail hinge, Asp24 (H4), and the patch center, Glu61 (H2A), located on two adjacent nucleosomes. The energy of the tail-patch interaction as a function of the distance is approximated by a smooth flat-well potential, where "E" defines the depth of the potential and "d = 35 Å" is the range of interaction. The energy calculated in this way corresponds to formation of one 'bridge' between two stacked nucleosomes. The optimal stacking between two nucleosomes involve two such bridges with the total energy "–E".

$$E_{tail-patch} = \frac{E}{4}\left(\frac{r-d}{1+|r-d|} - 1\right)$$

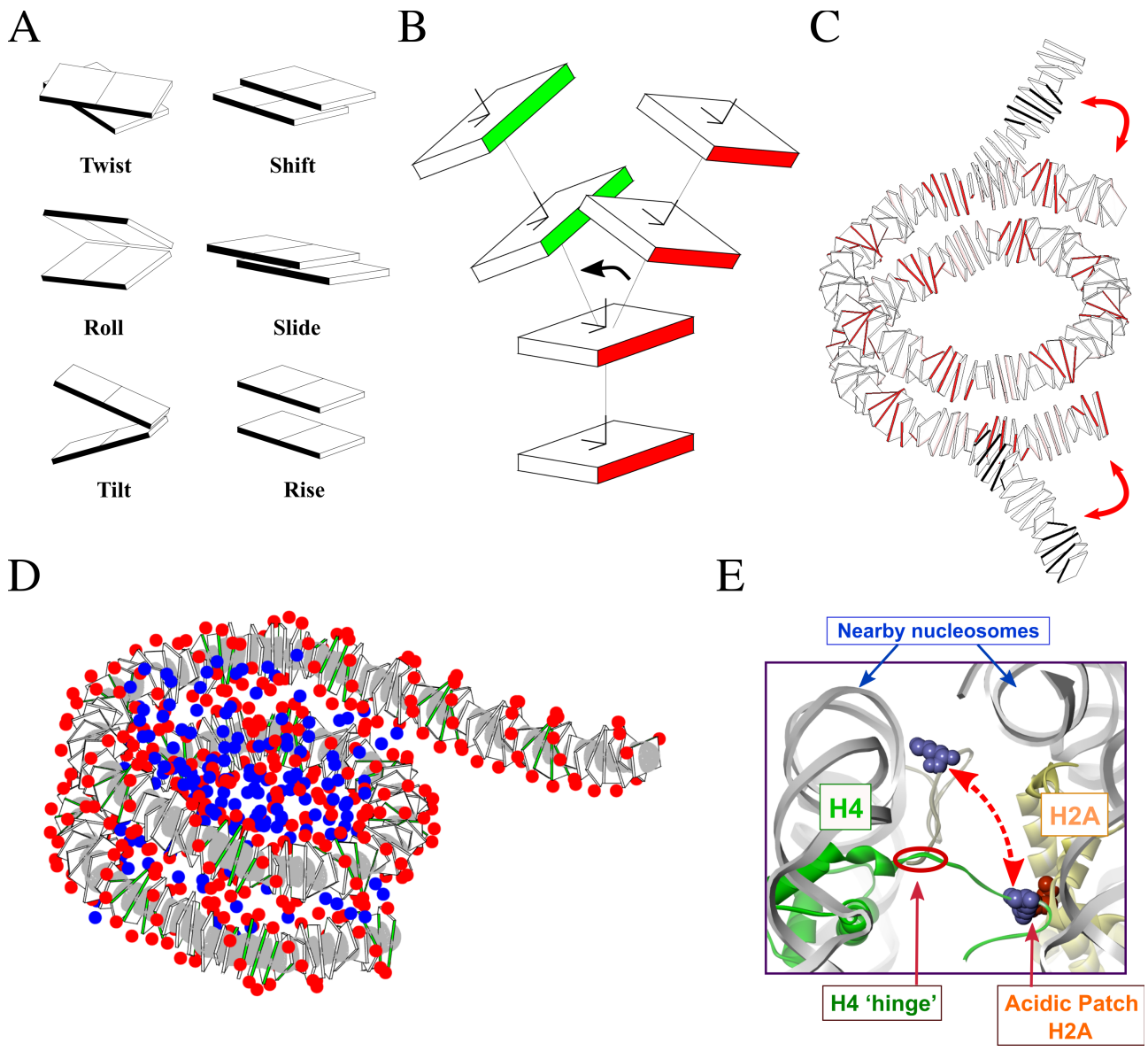

Figure S1. Schematic description of the DNA/fiber geometry, Monte Carlo moves, and energy terms. (**A**) Six base-pair step parameters define the geometry of DNA. Twist, Roll, and Tilt define the local twisting and bending of the DNA. Shift, Slide, and Rise determine the local shearing and stretching deformations (the minor groove sides of the base-pairs are shown in color). These parameters are related to the local base-pair coordinate frames according to a standard nomenclature devised in 1989 [S1]. The advantage of using this parameterization instead of utilizing only beads for the DNA is that it intrinsically includes the twist registry of the linker DNA that determines the relative orientation of the neighboring nucleosomes and the fiber topology [30], and also includes all the cross-correlation, sequence dependency, bending, and torsional flexibility terms in one single quadratic energy equation

[32]. The quadratic nature of this energy also allows us to initialize the conformation of the fiber using Gaussian sampling method [33].

(**B**) A typical Monte Carlo (MC) move is shown here. Six base-pair step parameters are updated in each move. The geometry of the linker DNA fluctuates around the regular B-DNA. The regular B-DNA parameters are [Twist, Tilt, Roll, Shift, Slide, Rise] = [34.5°, 0, 0, 0, 0, 3.35 Å] on average. In each MC step one base-pair step in one of the linkers (which include the unwrapped part of the nucleosomes (**C**) as well as the linker) is selected and the base-pair step parameters are changed randomly in the range of [δTwist, δTilt, δRoll, δShift, δSlide, δRise] = [±5°, ±3°, ±5°, ±0.3Å, ±0.5Å, ±0.2Å]. The range of values are chosen based on the rigidity matrix of deformations for DNA [32] to produce ~40% success rate for the MC step updates. The entire fiber "down-stream" of this change goes through a rigid body motion. In this figure, the second base-pair step is changed (as highlighted by the arrow). Thereby, the first two base pairs remain intact while the upper part is moved in space by some rotation and translation.

(**C**) Two nucleosome conformations, one with no unwrapping (red minor grooves) and one with U = 15 bp (black minor grooves) are shown. Unwrapping adds extra flexibility and extensibility to the fiber.

(**D**) To calculate electrostatic and van der Waals interactions, positive charges on arginines and lysines are considered (blue balls) as well as negative charges on aspartates, glutamates, and DNA phosphates (shown in red). All charges were partially neutralized to mimic the salt screening effects [30]. Large gray spheres assigned to the center of each base-pair are additional 'virtual' neutral atoms introduced to avoid the steric clashes with the DNA. After changing the base-pair step parameters and their local coordinate frames in each MC step, positions of the histones, centers of base pairs, and the phosphates are updated.

(**E**) During the course of simulations multiple stacking or H4 tail – acidic patch bonds are formed or broken down as nucleosomes change their relative surface to surface distance [30]. The depth of the potential is determined by the parameter "E" (see above).

Figures (A) to (D) are generated using MATLAB and figure (E) is generated by Accelrys Discovery Studio software.

Adhesion energy profile

In this section we derive a profile for the free energy of unwrapping, $G_{adh}(U)$, based on available force-spectroscopy data. Using dynamic force spectroscopy, Brower-Toland *et al.* [S5] estimated the free energy of unwrapping of the outer turn of DNA (U = 38 bp) as ~12 kcal/mol = 20 kT. Assuming that the adhesion energy is distributed uniformly over DNA, the energy per base pair is 0.26 kT/bp. This is consistent with the overall formation energy of nucleosomes estimated to be ~42 kT for 147 bp [S6] which gives the average adhesion energy per base pair ~0.28 kT/bp (Figure S2, red line).

To elucidate a detailed map of histone-DNA interactions along the DNA sequence with high precision, the mechanical unzipping of DNA from a single nucleosome 601 has been done by Hall *et al.* [12] using optical tweezers. The idea behind these experiments is that the dwell times measured at different DNA positions reflect the strengths of histone-DNA interactions at those positions. However, translating these dwell times into adhesion energy values is not straight-forward.

By treating the dwell times of DNA unwrapping measured by Hall *et al.* [12] as a Markov chain process, Forties *et al.* [S7] obtained an estimate for the adhesion energy landscape (black profile in Figure S2). For the initial stage of DNA unwrapping, $U \leq 28$ bp, they find the adhesion energy per base pair ~0.05 kT/bp (slope of the black curve at small U). The reason for this very small value is that Forties *et al.* chose the dwell time profile of the unzipping fork measured at the very high force F = 28 pN (Fig. 2 in [12]), with the dwell times being undetectable at the nucleosome ends. Their energy values are very low and predict a much more open '601' nucleosome than follows from Meng *et al.* force extension data [15] (simulation results with Forties *et al.* potential not shown).

Therefore, to estimate the adhesion energy of DNA, we used the unzipping traces measured at lower forces with the non-zero dwell times at the nucleosome ends (Fig. 3b in [12]). Our approach is based on the following assumptions: (1) Local unwrapping rate k_u is proportional to the inverse of the dwell time and relates to the adhesion energy, G_{adh}, by a Boltzmann factor: $k_u = 1/\tau = k_0 \exp(-G_{adh})$. (2) The rate constant k_0 is chosen so that the energy of unwrapping for the half of nucleosome (ΣG_{adh}) is ~20 kT [S6]. (3) If the dwell times are undetectable ($\tau \sim 0$) for certain DNA regions, we assign a minimum energy $G_{adh}^{min} = 0.13$ kT/bp, which is a half of the average adhesion value (see above).

Based on these assumptions, we calculated the green profile shown in Figure S2, which was used as the adhesion energy function, $G_{adh}(U)$, in our computations. This potential function allows the nucleosome ends to fluctuate between U = 0 and 20 bp at small forces F < 4 pN, with the average U varying between 8 and 15 bp depending on the external force (see Figures 5 and S8).

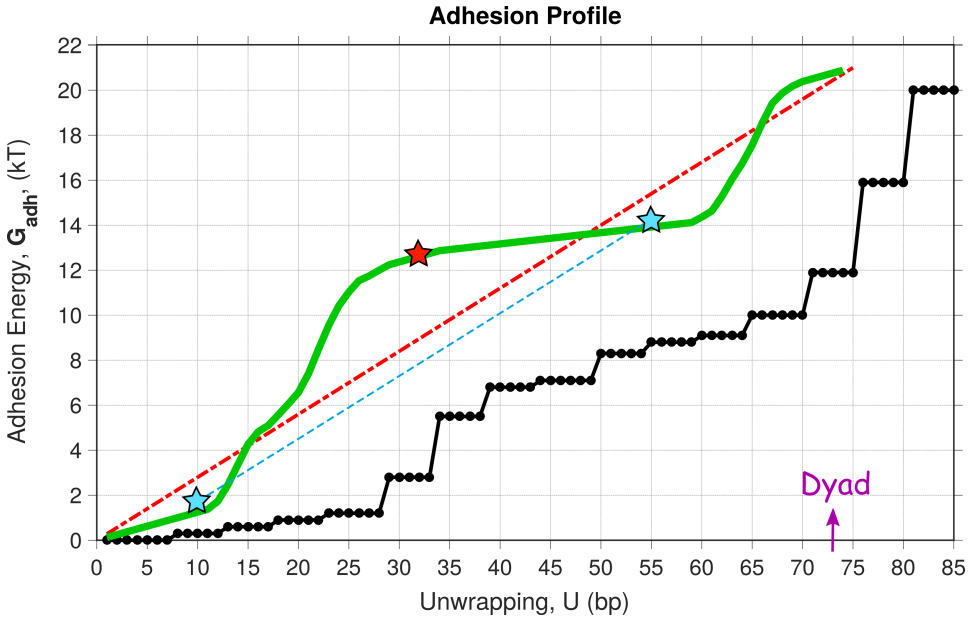

Figure S2: Adhesion energy as a function of nucleosomal DNA unwrapping. **Red**: Linear profile representing the average DNA-histones interactions (the slope 0.28 kT/bp). **Black**: Forties *et al.* [S7] translated the dwell time histogram obtained at high force F = 28 pN (Fig. 2 by Hall *et al.* [12]) into adhesion energy by implementing a Markov chain model. **Green**: Our estimate based on the average dwell times measured at low forces (presented in Fig. 3b by Hall *et al.* [12]). Importantly, this profile is lower than the average energy G_{adh} (red line) at some levels of unwrapping, while higher in other regions. By contrast, the Forties *et al.* profile remains lower than $G_{adh}(U)$ for any unwrapping U.

The curvature changes sign in the non-linear green profile. Notably, its central fragment locally concaves downward. This means that the central part of the graph lies above a line segment, dashed cyan, connecting the end points. This is important for understanding the structural origin of the bifurcation effect observed at high external forces $F \geq 4$ pN, when the average value $U = (U^L + U^R) / 2$ increases up to ~30 bp (Figures 5C and 5D).

Consider the following example. Let us assume that $(U^L + U^R) = 64$ bp. If the DNA unwrapping at both left and right ends of nucleosome is the same, $U^L = U^R = 32$ bp, the total adhesion energy is ~25 kT (which is two times the energy at the red asterisk shown in Figure S2). If, however, $U^L = 10$ bp and $U^R = 54$ bp, the total energy is ~16 kT (sum of the energies at the cyan asterisks shown in Figure S2). This simple example explains why it is more favorable to have a strong unwrapping $U \approx 55$ bp at one end, rather than to have 'intermediate' unwrapping $U \approx 30$ bp at the both ends of a nucleosome.

The region of steep increase in the adhesion energy (U = 15 – 25 bp) corresponds to the DNA positions where the arginines deeply penetrate into the minor groove of nucleosomal DNA [S8-S9]. Strong asymmetric unwrapping ensures that only one end of the nucleosome (the side with U ≈ 55 bp) pays to climb this energy barrier while the symmetric unwrapping requires twice as much energy. Importantly, as explained in the main manuscript, symmetric and asymmetric conformations generate similar Z_{ext} values.

In summary, the bimodal distribution of DNA unwrapping ($U^L \neq U^R$) helps decreasing the total adhesion energy under strong extension. In turn, this bimodality is a consequence of the specific shape of the adhesion energy profile, namely, its downward curvature at U ≈ 25 bp.

Simulation of unwrapping-rewrapping dynamics

Below, we describe the MC procedure used for simulation of spontaneous unwrapping-rewrapping of nucleosomal DNA. The nucleosome core particle is assumed to be fixed except for the unwrapped DNA, which is treated as a part of the "dynamic linker" DNA. The numbers of unwrapped base pairs at the Left and Right ends of a nucleosome are denoted U^L and U^R respectively (see the numbering scheme in Figure S3-A). The linker DNA is modeled at the level of base pairs and dimeric steps, and its trajectory is described by six dimeric step parameters [30, 32]. The dimeric steps and the base pairs are numbered in a conventional way, so that the step [i] describes transition from base pair (i) to base pair (i+1) [S1, 32].

In a single Monte Carlo step, we choose randomly a dynamic linker L_i (connecting nucleosomes N_i and N_{i+1}). Then, a dimeric step is selected from the following list of steps:

[145 – U^R – 1], **[145 – U^R]**, [145 – U^R + 1], …, [145], … [NRL], [1], [2], … **[U^L]**, **[U^L + 1]**

Here, the underlined steps belong to nucleosome N_{i+1}. The steps shown in magenta and blue are denoted in Figure S3-B by magenta and blue arrows, respectively. The magenta color indicates possible additional DNA unwrapping, while the blue color means that we either randomly change conformation of this dimeric step, or we perform a rewrapping move.

These are the three possible moves:

– (**Normal move**) If the selected dimeric step is not magenta or blue, its helical parameters are changed by the "six random increments" described in the Methods section and Figure S1. This move and the other ones (described below) include updating configuration of the nucleosome array, computing the "new" energy and performing the Metropolis acceptance test.

– (**Unwrapping move**) If the magenta dimeric step is selected, it is treated as the "newly unwrapped step". The helical parameters of this step are built using "six random increments" with the equilibrium B-DNA conformation as the starting point. If the new fiber conformation is accepted during the Metropolis test, then for the corresponding nucleosome

$$U^R \rightarrow U^R + 1 \quad \text{or} \quad U^L \rightarrow U^L + 1.$$

– (**Rewrapping move**) When the blue dimeric step is selected, it is treated as the "potentially rewrapping boundary step." With probability 50% it undergoes the "normal move" change, otherwise it rewraps (around the histone core). Rewrapping means restoring the helical parameters of DNA in the template nucleosome 601 in that position. Elastic energy of the newly wrapped DNA step is set to be zero. If the new fiber conformation is accepted, then for the corresponding nucleosome

$$U^R \rightarrow U^R - 1 \quad \text{or} \quad U^L \rightarrow U^L - 1.$$

The total adhesion energy of every nucleosome, $G_{adh}(U^R_i) + G_{adh}(U^L_i)$, is added to the total energy.

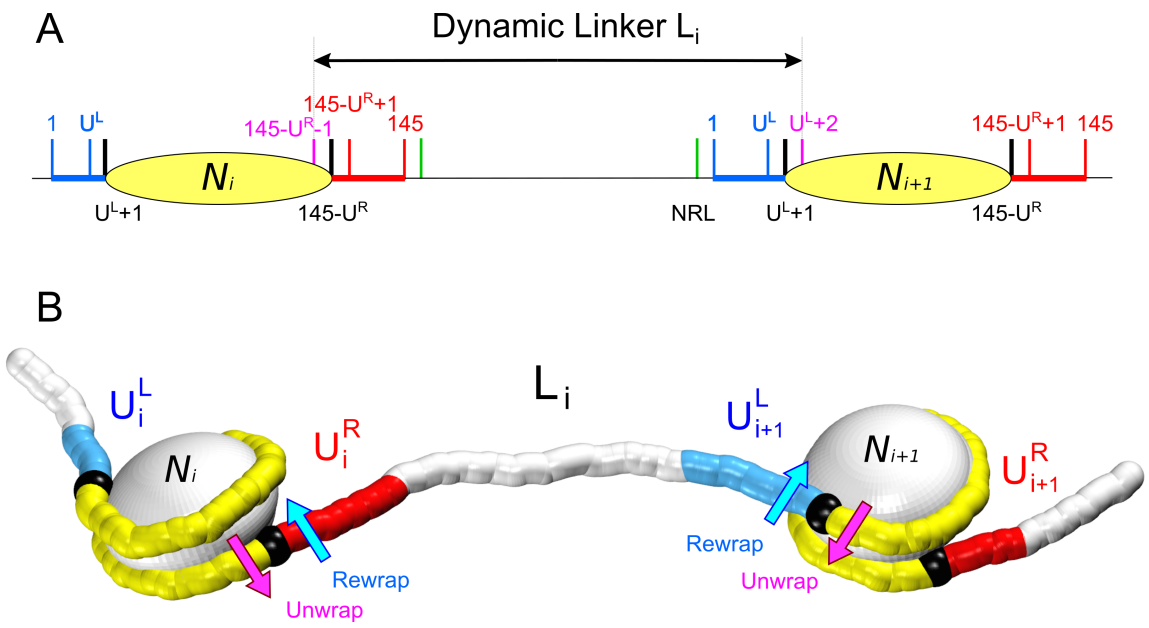

Figure S3: Schematic presentation of Monte Carlo procedure including dynamic unwrapping-rewrapping of nucleosomal DNA.

(A) Scheme explaining numbering of DNA base pairs. At the Left end, the base pairs 1, 2, … U^L are unwrapped; they are shown in blue. Similarly, at the Right end, the base pairs $145\text{-}U^R+1$, … 145 are unwrapped; they are shown in red. The yellow ovals represent DNA attached to histones; the boundary base pairs U^L+1 and $145\text{-}U^R$ are shown in black.

(B) Two adjacent nucleosomes N_i and N_{i+1} connected by dynamic linker L_i. The DNA attached to the histone core is shown in yellow, with the boundaries in black (consistent with (A)). The DNA unwrapped at the Left and Right ends of nucleosomes is colored in blue and red, respectively. The magenta arrows indicate additional DNA unwrapping, while the blue arrows denote a rewrapping move.

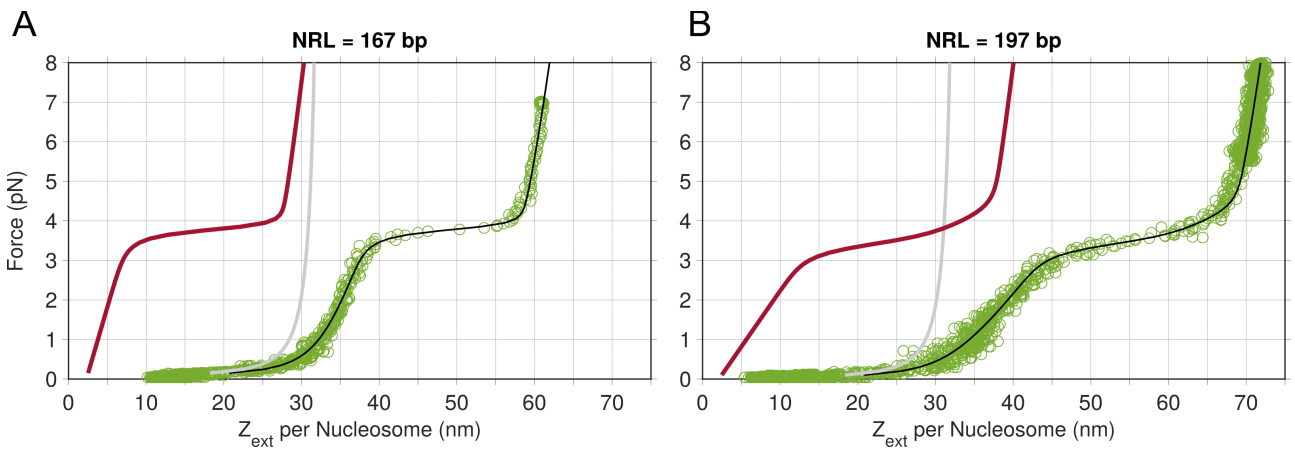

Figure S4. Extracting the force-extension response of the nucleosome arrays from raw experimental data kindly provided by J. van Noort (green circles). The force-spectroscopy measurements were performed by Meng *et al.* [15] for DNA containing 30 × 167 bp (A) and 15 × 197 bp repeats (B) of the Widom '601' nucleosome positioning sequence. To fit the data (which are normalized per nucleosome) we used the four-state model of chromatin fibers developed by Meng *et al*. [15]. The fitted curves are shown in black. The experimental setting involves 2035 bp-long DNA handles holding the nucleosome array between the surface of the flow cell and the magnetic bead. Note that, in practice with certain amount of free DNA attached to the flow cell surface or the magnetic tweezer bead, and several tetrasomes assembled on the handles, the effective length of the free DNA is considerably less than 2035 bp. The free DNA handles' response to the external force was estimated with a worm like chain (WLC) model, with the persistence length of 50 nm using the Meng *et al.* multi-state model [15]. Subtracting the WLC component (gray curves) from the black curves gives us the brown curves representing the net response of the nucleosome arrays.

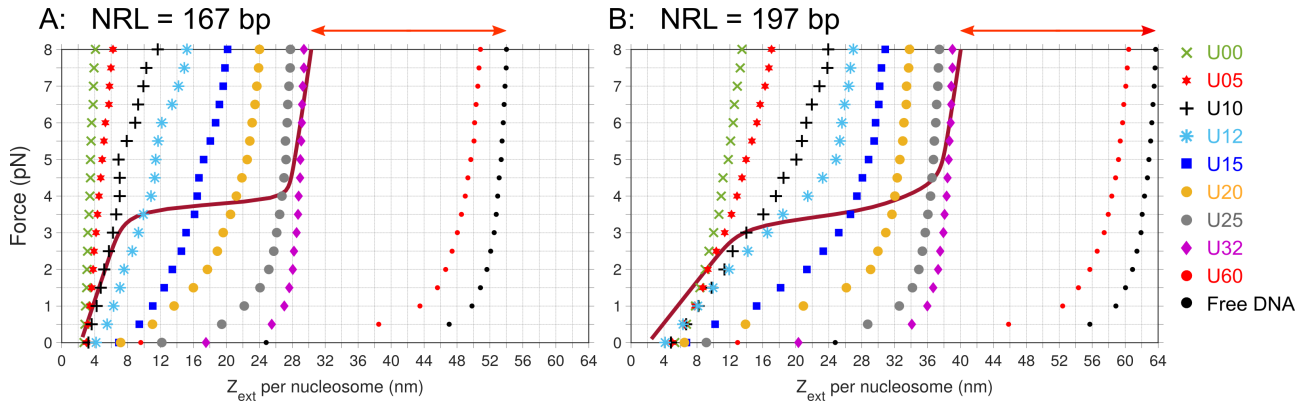

Figure S5. The force-extension profiles for the fibers with NRL = 167 bp (A) and 197 bp (B) obtained for different uniform unwrapping of nucleosomes, U, varying from 0 to 72 bp, and the stacking energy E = 0. The dotted lines (with various symbols) represent average extension per nucleosome obtained from MC simulations. The solid curves show experimental data [15]. This figure includes the data of Figure 2 plus U = 5, 60, and 72 bp cases. The red arrows represent the difference in Z_{ext} between U = 32 bp and U = 72 bp (free DNA): the 24 ± 1.0 nm extension corresponds to the inner-turn unwrapping of nucleosomes (F = 8 pN, NRL = 167 and 197 bp). This is very close to the values measured by Meng *et al*., 24 ± 8 nm and 24 ± 7 nm for NRL = 167 and 197 bp, respectively [15]. At small U and small force the force-extension curve is linear while at U = 25 – 72 bp, the force-extension dependence resembles a WLC polymer response.

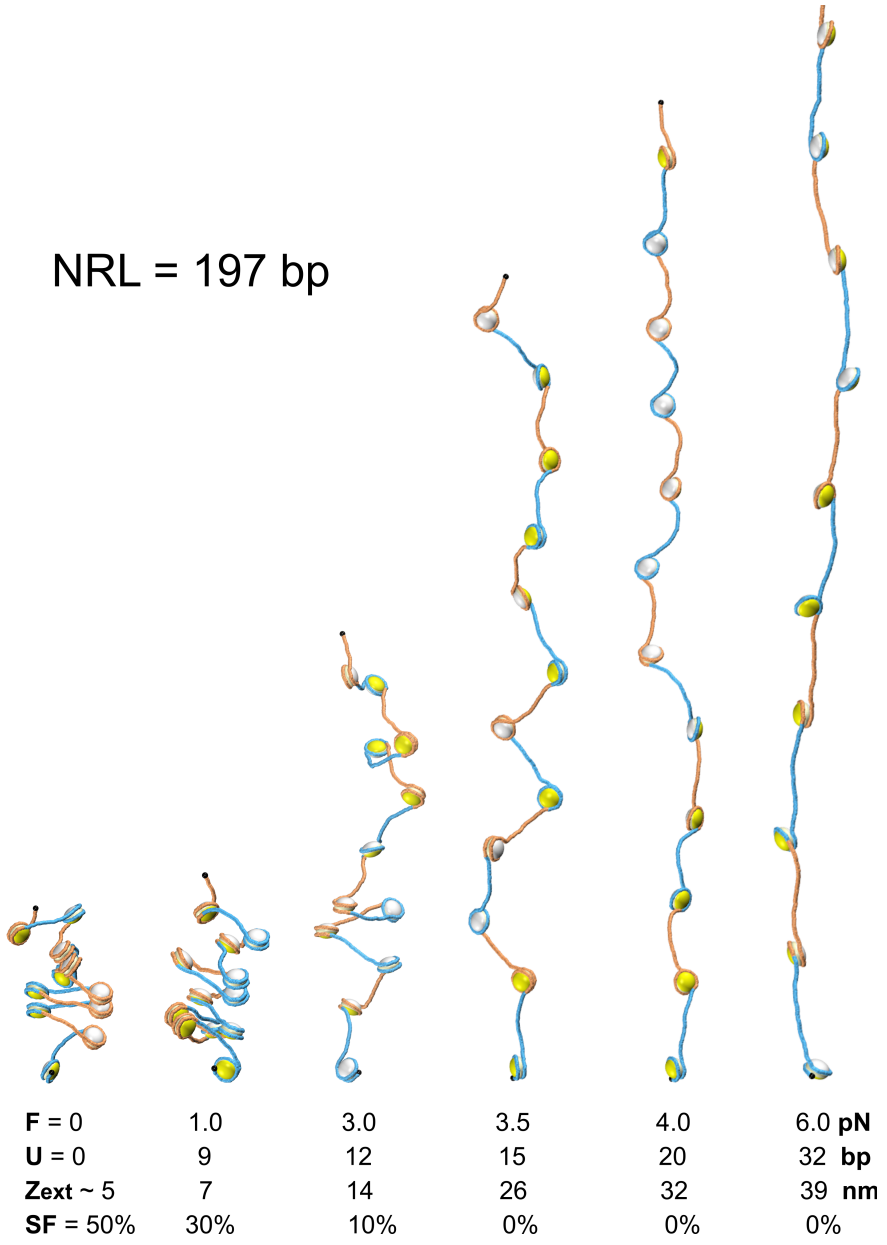

Figure S6. Typical conformations of the chromatin fiber with NRL = 197 bp simulated for the external force increasing from F = 0 to 8 pN. At small forces F ≤ 3.0 pN the DNA unwrapping is insignificant, U ≤ 12 bp, and the fiber remains relatively compact despite numerous stacking-unstacking events. With the increase in applied force, the unwrapping of nucleosomal DNA becomes much stronger and goes up to U = 20 bp at F = 4 pN, and up to U = 32 bp at F = 8 pN. These MC simulations were performed for the stacking energy E = 8 kT. At F = 3.5 pN and higher, the inter-nucleosome stacking is lost completely. The force-unwrapping, force-extension, and force-unstacking dependencies are presented at the bottom. See also the Supplementary Movies.

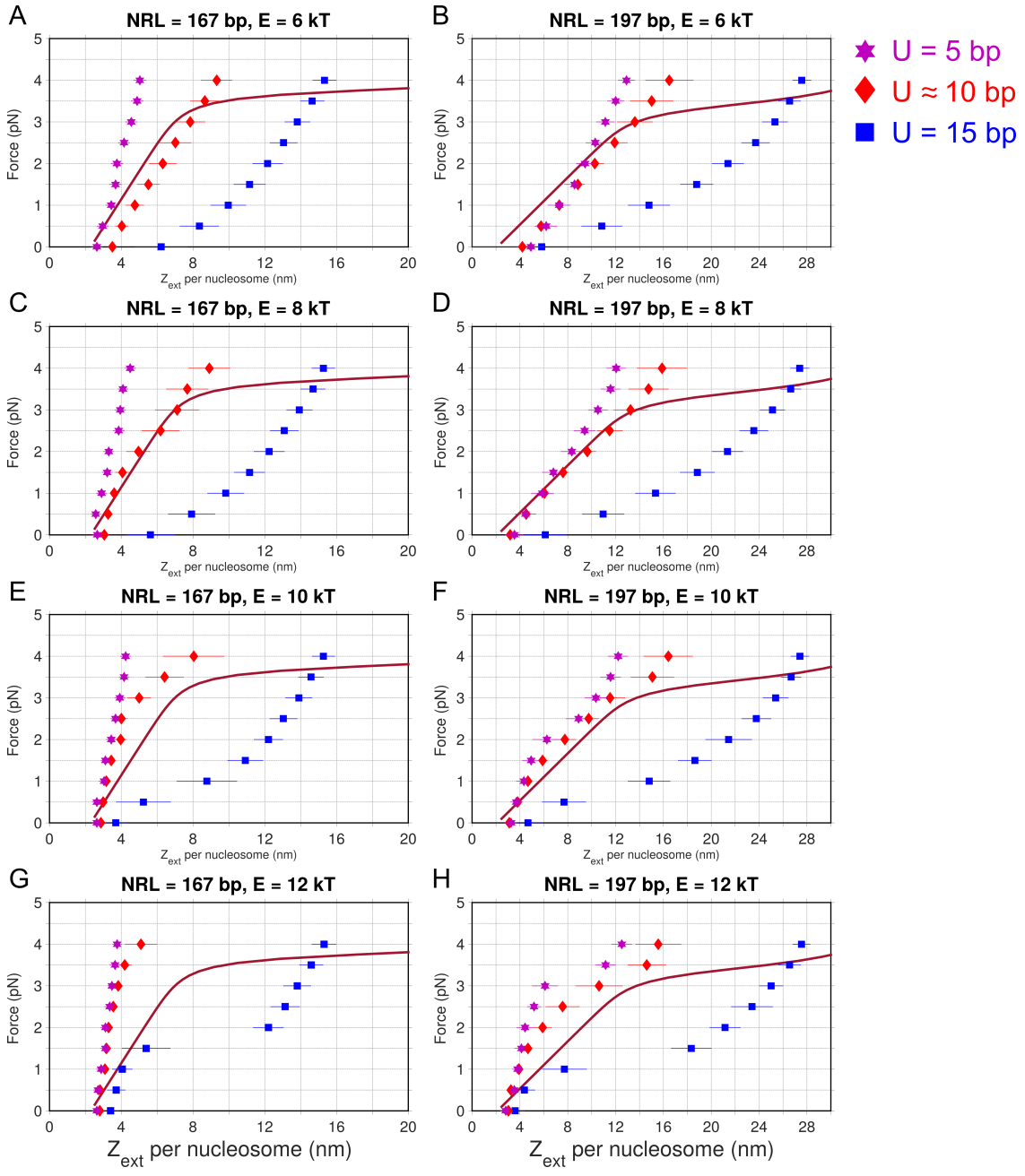

Figure S7. Selecting the optimal parameters (unwrapping, U, and stacking energy, E) accounting for the experimental observations (solid lines). In our MC simulations, we systematically changed U from 5 to 15 bp and E from 6 to 12 kT for both NRL = 167 and 197 bp. The fibers with U = 15 bp are excluded from further consideration since they do not show a linear behavior at small forces (A, B: E = 6 kT and U = 15 bp) and increasing the stacking energy does not produce the stable linearity we seek (G, H: E = 12 kT and U = 15 bp). Stacking energy E = 6 kT is too low and cannot generate the

experimentally observed extensions for NRL = 197 bp (B). Stacking energy E = 12 kT is too high and no MC calculated curves coincide with the experiment (G, H). Stacking energy E = 10 kT is too high for NRL = 167 bp (E). Thus, we find that E = 8 kT is the optimal energy value: it stabilizes a linear regime with U ≈ 10 bp (more specifically, U = 10 – 12 bp for NRL = 167 bp and U = 9 – 12 bp for NRL = 197 bp, at F ≤ 3.0 pN). To reach the observed extensions in the plateau region, nucleosomes must unfold beyond this initial unwrapping at intermediate forces. All stacks are disrupted at force F = 3.5 – 4.0 pN, and unwrapping U increases from 12 to 25 bp in this force regime.

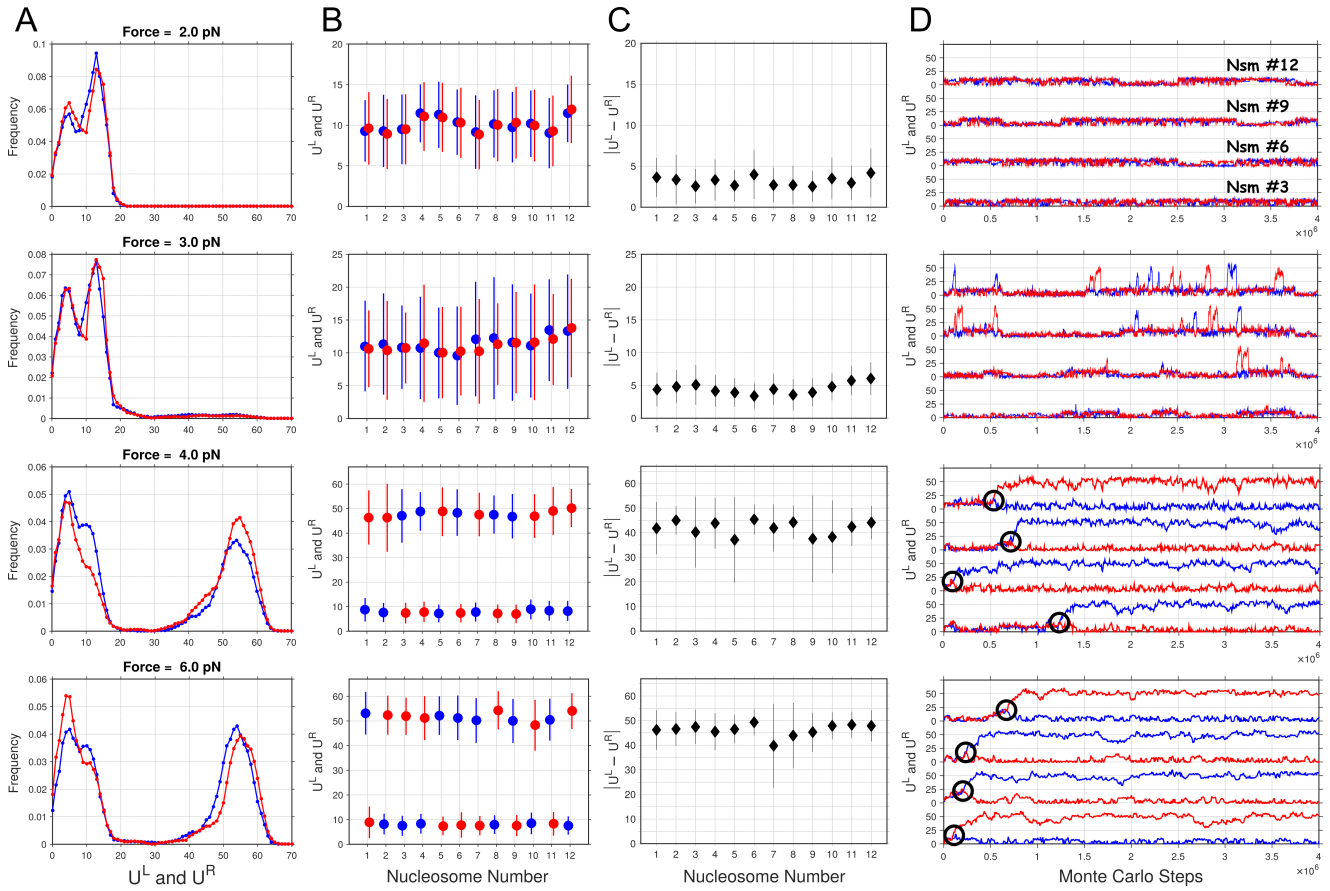

Figure S8. Spontaneous unwrapping of nucleosomal DNA during MC simulations.

The data are presented for the 167 × 12 nucleosome array; external force varies from 2.0 to 6.0 pN.

Column (A). The histograms for DNA unwrapping at the left and right ends of nucleosomes, U^L (blue) and U^R (red), are shown. At forces below 4.0 pN, the DNA unwrapping mostly remains within a narrow interval from 0 to 20 bp. At forces $F \geq 4.0$ pN, the distribution of DNA unwrapping becomes bimodal, with one peak corresponding to the U^L and U^R values less than 20 bp, and the second peak, to unwrapping of 55 (±10) bp. This bifurcation occurs due to the locally concave profile of the adhesion potential (Figure S2).

Column (B). The averages and fluctuations of U^L and U^R for 12 individual nucleosomes are presented. At the forces F = 2.0 and 3.0 pN, for each nucleosome the U^L and U^R values are nearly identical. The unwrapping is somewhat stronger for the terminal nucleosomes #1 and #12 (compared to the internal nucleosomes #2 to #11), but this difference of ~2 bp is insignificant. At F = 3.0 pN, the fluctuations of U^L and U^R are higher than at F = 2.0 pN, which is consistent with occasional DNA unwrapping (up to 55 bp) observed at F = 3.0 pN. At the forces F = 4.0 and 6.0 pN, the two sets of the U^L and U^R values correspond to the two unwrapping branches presented in the histograms.

For example, at F = 6.0 pN, in nsm #3 and nsm #12 the red circles and bars (U^R) are on the top, indicating that the unwrapping occurred at the right ends of these nucleosomes. Accordingly, in the right panel, in nsm #3 and nsm #12 the red trajectories are on the top.

On the other hand, in nsm #6 and nsm #9 the blue circles (U^L) are on the top, which is consistent with the blue trajectories #6 and #9 being on the top in the right panel.

Column (C). The absolute difference between U^L and U^R for individual nucleosomes is a direct measure of unwrapping asymmetry. The ensemble averages and standard deviations of $|U^L - U^R|$ values for all nucleosomes in the 12-mer array are presented here. At low forces, $F \sim 0 - 3$ pN, the asymmetry of unwrapping does not exceed 4 – 5 bp. At $F \geq 4.0$ pN, this value increases up to 40 – 45 bp.

Column (D). The trajectories visualizing evolution of the U^L and U^R values during the first 4 million MC steps are presented for selected nucleosomes (#3, #6, #9 and #12). Consistent with the histograms on the left, at forces $F < 4.0$ pN, the U^L and U^R values fluctuate between 0 and 20 bp. Rare occurrences of strong DNA unwrapping (up to 55 bp) in isolated nucleosomes are observed at F = 3.0 pN. At forces $F \geq 4.0$ pN, the trajectories divide in two branches – one remains between 0 and 20 bp, and the other goes up to 40-60 bp. The bifurcation points are emphasized by the black circles.

In summary, U^L and U^R, fluctuate independently and branch off at high forces. We don't observe any cooperativity in the asymmetric unwrapping of neighboring nucleosomes, that is, the left and right arms of adjacent nucleosomes unwrap independently. This reflects the stochastic nature of the nucleosome opening.

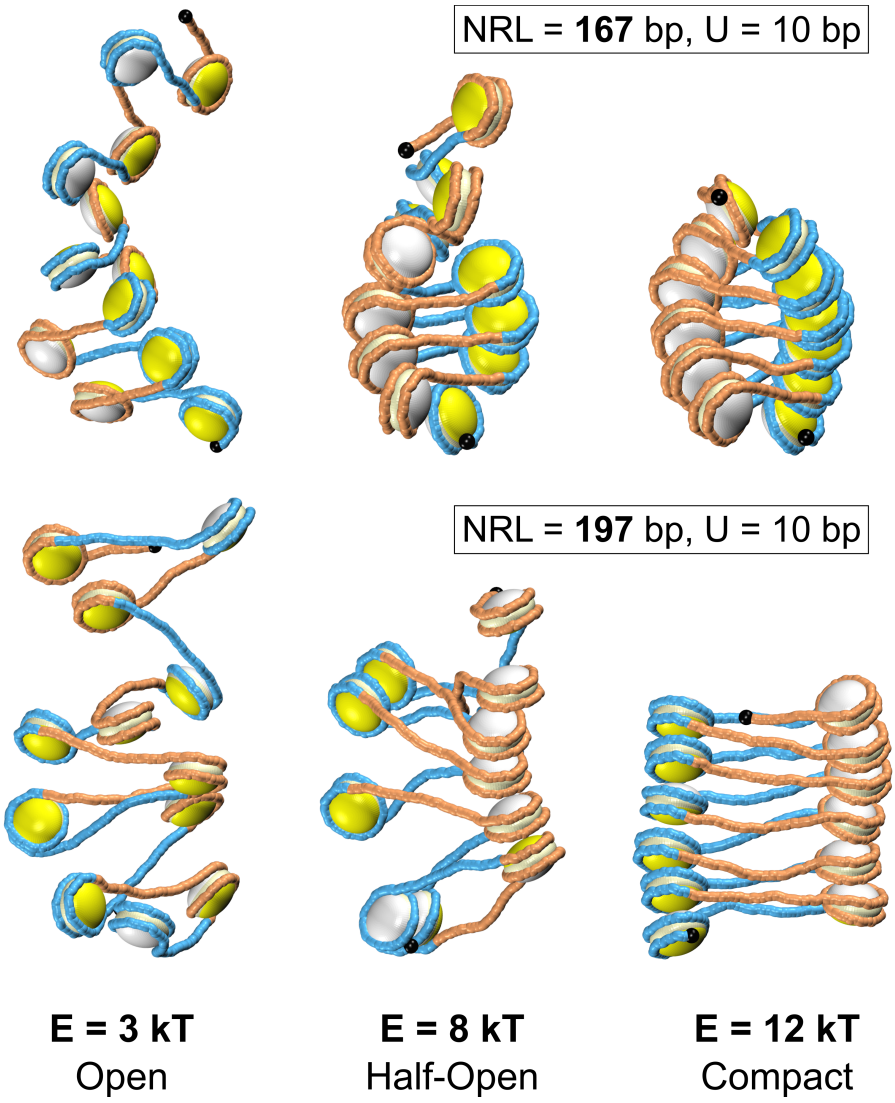

Figure S9. Representative fiber conformations for E = 3 kT (open), 8 kT (half-open), and 12 kT (compact) are shown at zero external force. The MC-simulated conformations largely resembled two-start packing, with rare events of three- to five-start morphologies. We don't observe solenoid (one-start) stacking folds. Our computations suggest that the range of energies for unstacked chromatin is E ≈ 0 – 3 kT, while E ≥ 12 kT condenses the fiber. Intermediate energy values, E ≈ 8 kT, represent chromatin randomly opening and closing under thermal fluctuations.

References:

S1. Dickerson, R. E., M. Bansal, C. R. Calladine, …, A. H. -J. Wang, and V. B. Zhurkin. 1989. Definitions and nomenclature of nucleic acid structure parameters. *EMBO J*. 8:1-4.

S2. Hewish, D. R. and L. A. Burgoyne. 1973. Chromatin sub-structure. The digestion of chromatin DNA at regularly spaced sites by a nuclear deoxyribonuclease. *Biochem Biophys Res Commun.* 52:504-510.

S3. Materese, C. K., A. Savelyev, and G. A. Papoian. 2009. Counterion atmosphere and hydration patterns near a nucleosome core particle. *J Am Chem Soc.* 131:15005-15013.

S4. Shaytan, A.K., G.A. Armeev, A. Goncearenco, V.B. Zhurkin, D. Landsman , and A.R. Panchenko. 2016. Coupling between histone conformations and dna geometry in nucleosomes on a microsecond timescale: atomistic insights into nucleosome functions. *JMB*. 428:221-237.

S5. Brower-Toland, B. D., C. L. Smith, R. C. Yeh, J. T. Lis, C. L. Peterson, and M. D. Wang. 2002. Mechanical disruption of individual nucleosomes reveals a reversible multistage release of DNA. *Proc. Natl. Acad. Sci. U.S.A.* 99:1960-1965.

S6. Ranjith, P., J. Yan , and J. F. Marko. 2007. Nucleosome hopping and sliding kinetics determined from dynamics of single chromatin fibers in xenopus egg extracts. *Proc Natl Acad Sci USA*. 104:13649.

S7. Forties, R. A., J. A. North, S. Javaid, O. P. Tabbaa, R. Fishel, M. G. Poirier, and R. Bundschuh. 2011. A quantitative model of nucleosome dynamics. *Nucleic Acids Research*. 39:8306-8313.

S8. Rohs, R., S. M. West, A. Sosinsky, P. Liu, R. S. Mann, and B. Honig. 2009. The role of DNA shape in protein-DNA recognition. *Nature*. 461:1248.

S9. Wang, D., N. B. Ulyanov, and V. B. Zhurkin. 2010. Sequence-dependent Kink-and-Slide Deformations of Nucleosomal DNA Facilitated by Histone Arginines Bound in the Minor Groove. *J. Biomol. Struct. Dyn*. 27:843-859.